V51B-0537 2004 AGU FALL MEETING

PREDICTION OF EMPEROR-HAWAII SEAMOUNT LOCATIONS FROM A REVISED MODEL OF GLOBAL PLATE MOTION AND MANTLE FLOW: 1. METHOD

Institute of Geological & Nuclear Sciences Limited

Rupert Sutherland
Institute of Geological and Nuclear Sciences,
PO Box 30-368, Lower Hutt,
New Zealand
r.sutherland@gns.cri.nz

Bernhard Steinberger
Institute for Frontier Research on Earth Evolution (IFREE),
Japan Marine Science & Technology Center (JAMSTEC)
2-15 Natsushima-cho, Yokosuka, 237-0061 Japan
Now at: Geological Survey of Norway, N-7491 Trondheim, Norway
bernhard.steinberger@ngu.no

Richard J. O'Connell
Dept. of Earth & Planetary Sciences,
Harvard University,
20 Oxford St., Cambridge MA 02138, USA
oconnell@geophysics.harvard.edu

Concept:

Physical model of mantle
Assume relationship between density, temperature, depth, and seismic velocity.
Viscosity model from Geoid and heat flow.

Predict present velocity field and past flow
Global plate motions and past locations of plate boundaries used as constraints in flow computation.

Implant plumes at arbitrary time & place
Advection of plume conduits by large-scale flow and vertical buoyant rising.
Fix to base of mantle or freely move.

Compute trace of plume at base of lithosphere
Iterate plume emplacement to optimise fit between predictions and known hotspot geology, and hence tie plate-motion model to mantle reference frame.

Radial Mantle Viscosity structure $\eta(z)$

Stress-strain relationship $\dot{\varepsilon} = C_1 \sigma^n exp\left(-\frac{H}{RT}\right)$

$$\Longrightarrow \eta(z) = \eta_0 \exp\left(\frac{H(z)}{nR\bar{T}(z)}\right) \cdot \left(<\dot{\epsilon}^2>(z)\right)^{\frac{1-n}{2n}}$$

η_0 (may be different for upper mantle, transition zone, lower mantle) to be determined by optimizing fit to various observables (geoid, heat flux, CMB excess ellipticity ...)

H = activation enthalpy T = temperature

Empirical relationship: $H = gRT_m$, T_m = melting temperature

Here use $g/n = 12$ (Yamazaki and Karato, 2001)

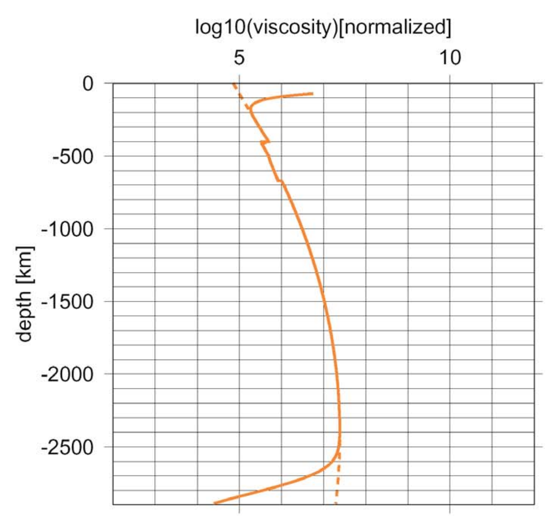

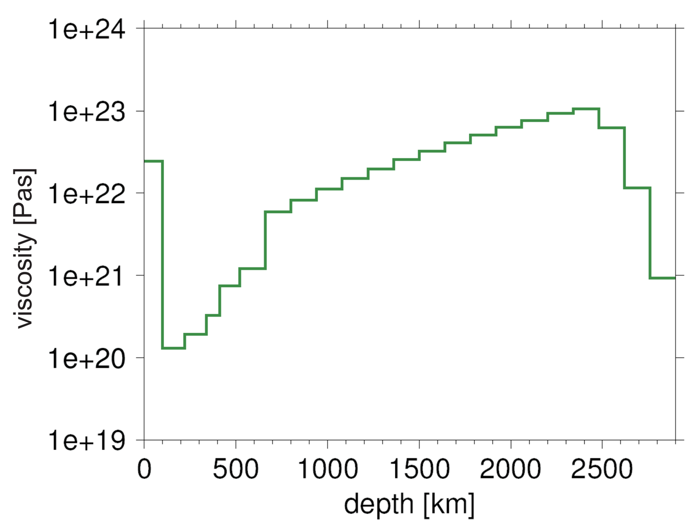

Obtained from optimizing fit to geoid, with additional heat flow constraint (Steinberger and Calderwood, 2001)

Thermal expansivity profile

Integrate $\frac{d\ln\alpha}{d\ln\rho} = -\delta_T$ along isotherms.

Upper mantle: $\delta_T = 5.5$; formalism by Schmeling et al. (2003).

Lower mantle: $\delta_T = \delta_{T0}\left(\frac{\rho_0}{\rho}\right)^b$

$\delta_{T0} = 5.5$ and $b = 1.4$

$\alpha_0(T) = (35 + 9T/1000\text{K}) \cdot 10^{-6}\text{K}^{-1}$ for zero pressure

$\rho(z)$ from PREM, $\rho_0(z)$ from evaluating PREM lower mantle parameters at z=0 and accounting for temperature difference.

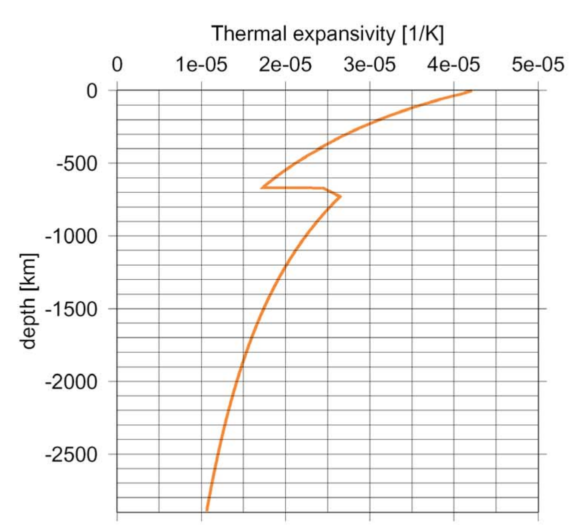

Radial Mantle Temperature profile

Adiabatic temperature profile $T(z)$ obtained by integrating

$$\frac{dT}{dz} = T(z) \cdot \alpha(z) \cdot g(z)/C_p(z).$$

$g(z)$ = gravity, $\alpha(z)$ is thermal expansivity

$C_p \approx 1250\text{J kg}^{-1}\text{K}^{-1}$ is specific heat

black line: Melting temperature profile (Wang, 1999; Zerr and Boehler, 1994; Yamazaki and Karato, 2001)

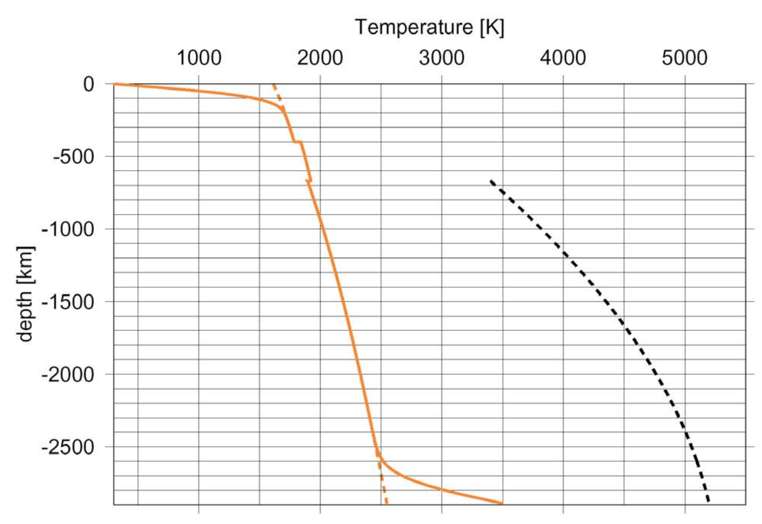

Mantle density anomalies

Seismic velocity anomalies δv_s from tomography

Assume thermal origin of δv_s and density anomalies $\delta\rho$:

$F_{s,th} := (\delta\rho/\rho)/(\delta v_s/v_s) = (\alpha/\rho)/(\partial \ln v_s/\partial T)_p$

Orange line: g=12; Red line: g=27; Purple line: g=42

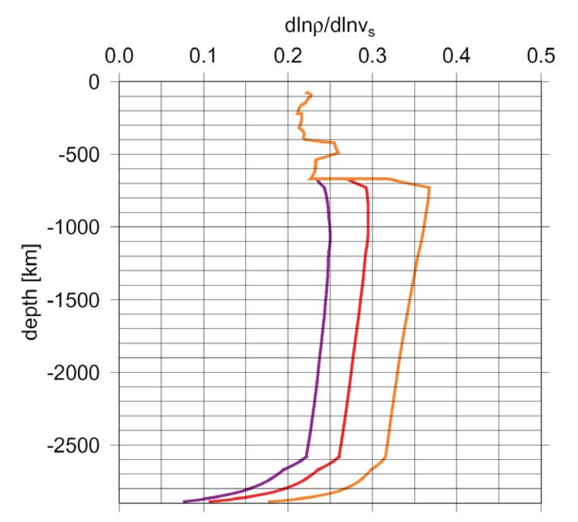

Relate seismic velocity and temperature anomalies

Include anelastic and anharmonic effects:

$$-(\partial \ln v_s/\partial T)_p = -(\partial \ln v_{s,0}/\partial T)_p + (Q^{-1}/\pi)\cdot(gT_m/T^2)$$

Dashed line: Anharmonic part. In the upper mantle after Goes et al. (2004); In the lower mantle, compute $\mu(T, z)$ by integrating

$$\frac{d\mu}{dz}(T_0(z) \pm \Delta T(z)) = \frac{d\mu}{dz}(T_0(z))(1 \pm \alpha(z)\Delta T(z)) \quad (1)$$

(Duffy and Anderson, 1989). Starting point is

$$\mu(T_0(z_0) \pm \Delta T(z_0)) = \mu(T_0(z_0)) \pm \Delta T(z_0) \cdot \frac{d\mu_0}{dT}$$

$\frac{d\mu_0}{dT}$=27 MPa/K; $\frac{d\mu}{dz}(T_0(z))$ and $\mu(T_0(z_0))$ from PREM.
Dotted lines: Anelastic part. Continuous: Total
Orange lines: g=12; Red lines: g=27; Purple lines: g=42

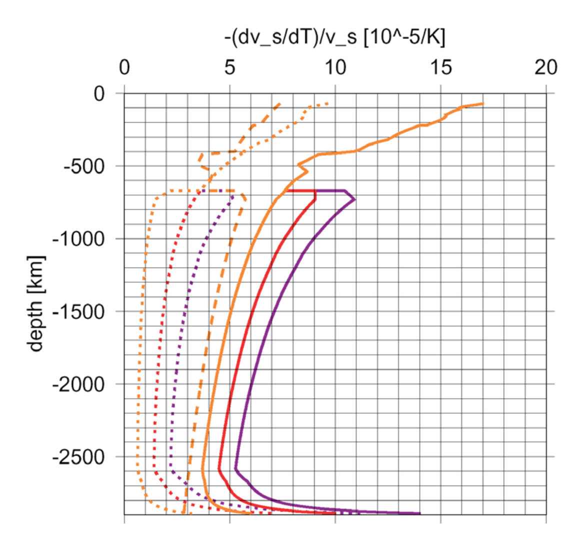

Global plate-motion chains

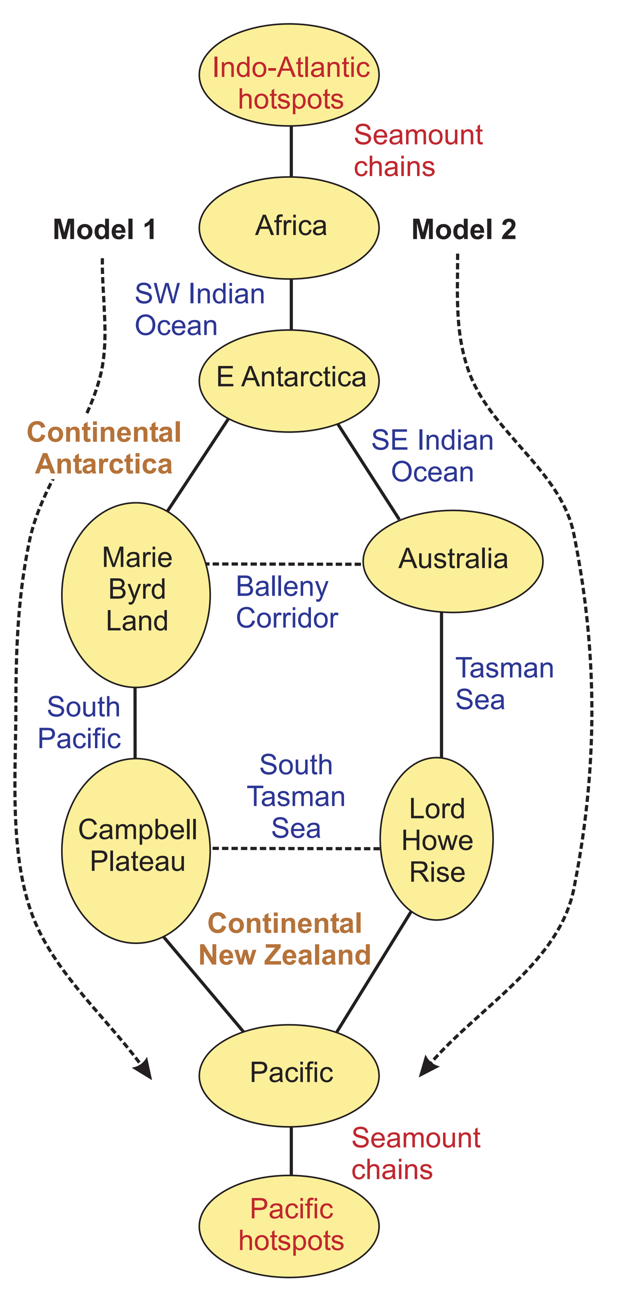

Relative plate motion chains for times older than chron 20 (43 Ma). For times <43 Ma both models follow a chain through continental Antarctica, and include motion from Cande et al. (2000).

South Pacific plate-motion circuit

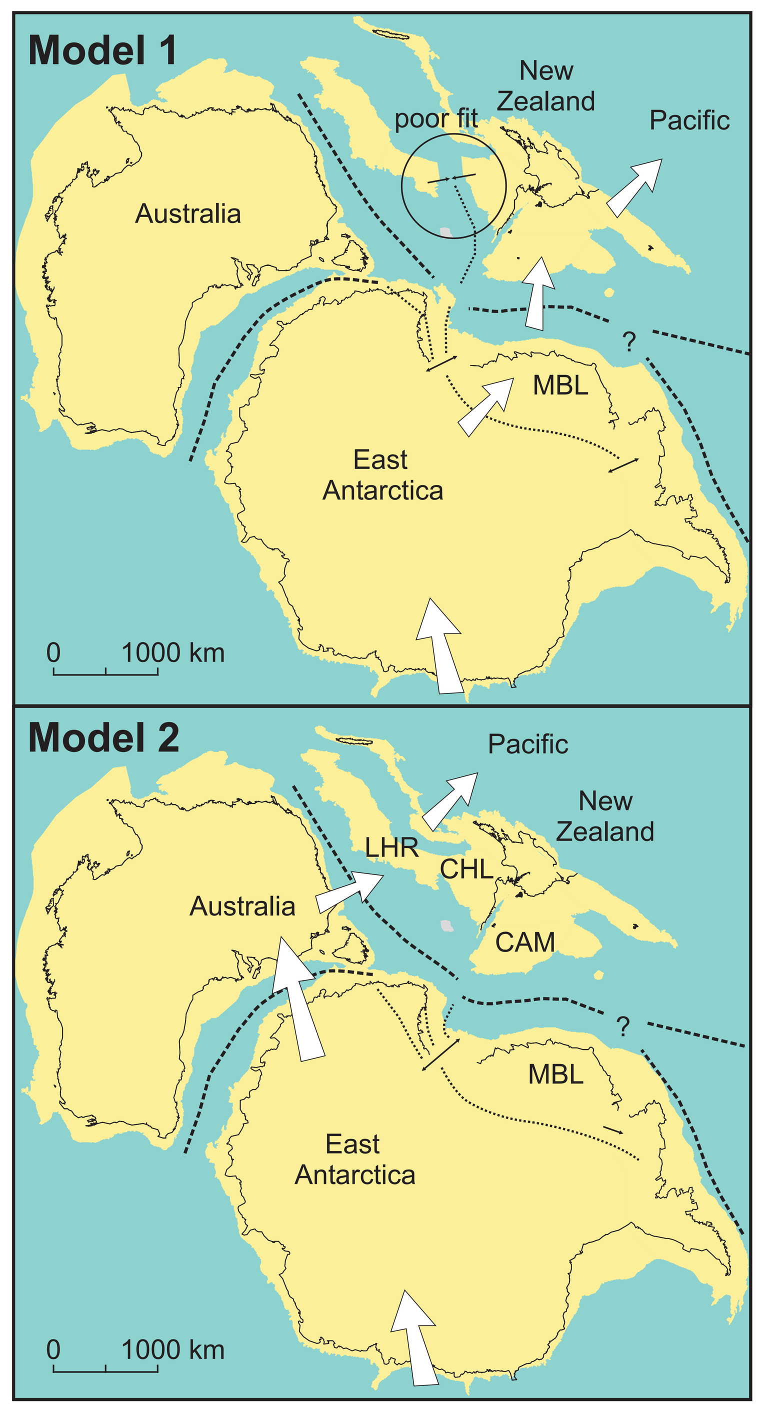

68 Ma reconstructions showing implications of alternate plate-motion chains (83-43 Ma). Black arrows are scaled to be double the convergence in New Zealand (68-43 Ma), or rifting in Antarctica (68-26 Ma), that is predicted through closure of the South Pacific plate-motion circuit. Model 2 is in much better accord with local observations.

Additional Cretaceous intra-plate deformation?

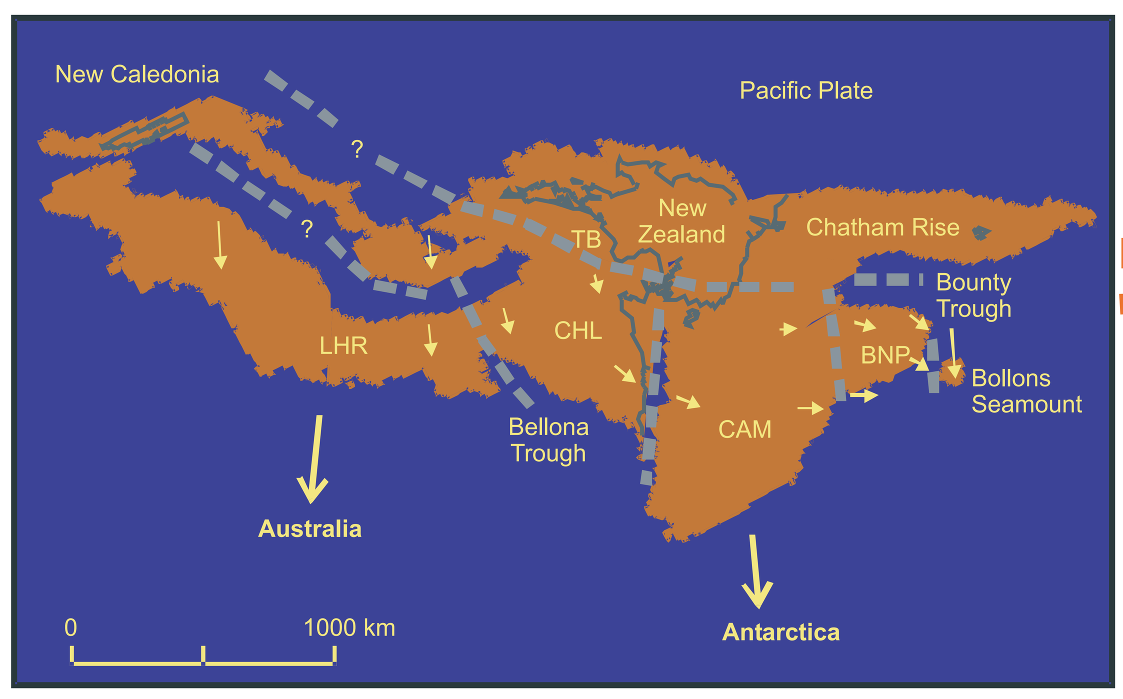

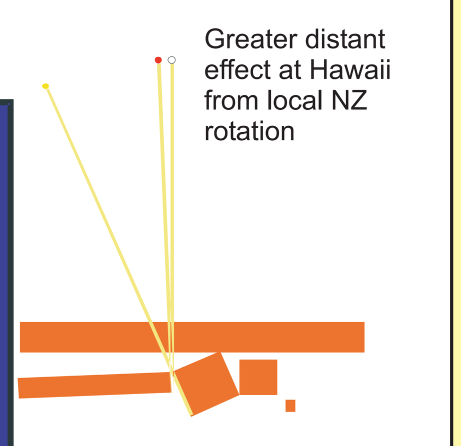

Although NOT incuded in this analysis, additional intra-plate rifting that may affect both plate motion chains is suggested by New Zealand geology. Rifting is likely to have continued in places until chron 33 (79-74 Ma) and may have locally continued until as late as 60 Ma. Forward models show that implied block rotations have approximately the right geometry to improve our fit to the oldest part of the Emperor chain. The much greater local rotation of the Campbell Plateau, as compared to the long and thin Lord Howe Rise and New Caledonia Basin, means that model 1 is most severely affected by Cretaceous rifting.

REFERENCES

Becker, TW and L. Boschi. 2002. A comparison of tomographic and geodynamic mantle models, Geochem. Geophys. Geosyst., 3, 2001GC000168.
Cande, S.C.; Stock, J.M.; Mueller, R.D.; Ishihara, T. 2000: Cenozoic motion between East and West Antarctica. Nature 404: 145-150.
Duffy, T.S., and Anderson, D.L., 1989. Seismic velocities in mantle minerals and the mineralogy of the upper mantle, J. Geophys. Res., 94, 1895-1912.
Goes, S., Cammaranoa, F., and Hansen, U., 2004. Synthetic seismic signature of thermal mantle plumes, Earth Planet. Sci. Lett., 218, 403-419.
Hager, B. H., O'Connell, R. J., 1979. Kinematic models of large-scale flow in the Earth's mantle, Journal of Geophysical Research, 84 (B3), p. 1031-1048.
Hager, B. H., O'Connell, R. J. 1981. A simple global model of plate dynamics and mantle convection. Journal of Geophysical Research. B, 86 (6), p. 4843-4867.
Schmeling, H., Marquart, G., and Ruedas, T., 2003. Pressure- and temperature-dependent thermal expansivity and the effect on mantle convection and surface observables, Geophys. J. Int., 154, 224-229.
Steinberger, B. M., and A. R. Calderwood, Mineral physics constraints on viscous flow models of mantle flow, J. Conf. Abs., 6, 2001.
Tarduno, J.A., R.A. Duncan, D.W. Scholl, R.D. Cottrell, B. Steinberger, T. Thordarson, B.C. Kerr, C.R. Neal, F.A. Frey, M. Torii and C. Carvallo (2003). The Emperor Seamounts: Southward motion of the Hawaiian hotspot plume in Earth's mantle, Science, 301, 1064-1069.
Wang, Z.W. 1999. The melting of Al-bearing perovskite at the core-mantle boundary. Phys. Earth Planet. Inter. 115: 219-228.
Yamazaki, D. and Karato, S., 2001. Some mineral physics constraints on rheology of Earth's lower mantle. Amer. Mineral., 86: 385-391.
Zerr, A. and Boehler, R. 1994. Constraints on the melting temperature of the lower mantle from high pressure experiments on MgO and magnesiowustite. Nature, 371, 506–508.

Details of other sources used are given in:
Steinberger, B., Sutherland, R., O'Connell, R.J. 2004. Prediction of Emperor-Hawaii seamount locations from a revised model of global plate motion and mantle flow. Nature 430: 167-173.

Prediction of Emperor-Hawaii Seamount Locations From a Revised Model of Global Plate Motion and Mantle Flow: 2. Results & Conclusions

Institute of Geological & Nuclear Sciences Limited

Rupert Sutherland
Institute of Geological and Nuclear Sciences,
PO Box 30-368, Lower Hutt,
New Zealand
r.sutherland@gns.cri.nz

Bernhard Steinberger
Institute for Frontier Research on Earth Evolution (IFREE),
Japan Marine Science & Technology Center (JAMSTEC)
2-15 Natsushima-cho, Yokosuka, 237-0061 Japan
Now at: Geological Survey of Norway, N-7491 Trondheim, Norway
bernhard.steinberger@ngu.no

Richard J. O'Connell
Dept. of Earth & Planetary Sciences,
Harvard University,
20 Oxford St., Cambridge MA 02138, USA
oconnell@geophysics.harvard.edu

Conclusions (Nature 430: 167-173)

Hotspot motion predicted by model of mantle flow improves fit for times <43 Ma

Predicted hotspot motion improves fit to Emperor seamount paleolatitudes 49-80 Ma, but does not improve longitude misfit

Plate motions uncertain before 43 Ma: 'missing' boundary in S Pacific

Model 1, no intra-Antarctic boundary before 43 Ma, produces poor fit to Emperor seamounts, and predicts convergence in New Zealand - inconsistent with rift structure

Model 2, no Tonga-Kermadec boundary before 43 Ma, produces a better fit to Emperor seamounts, and acceptably predicts Antarctic rift structure

Hotspot motion AND 'missing' intra-plate deformation are required to explain global observations of seamounts related to deep-seated hotspots

Computed flow field

Based on model smean by Becker and Boschi (2002)
$(\delta\rho/\rho)/(\delta v_s/v_s)$=0.2 below 220 km
→ 2 cm/yr

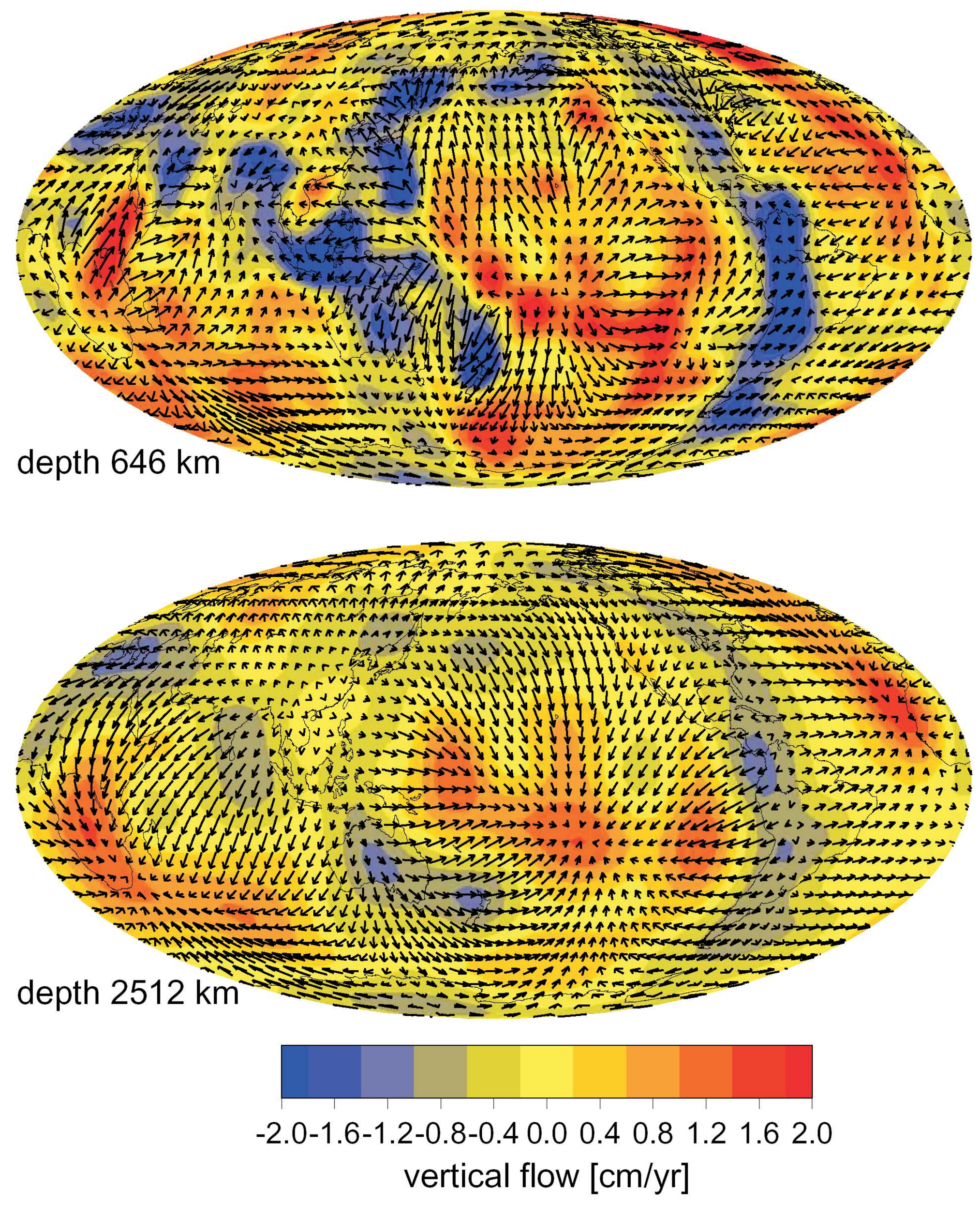

N-S mantle cross section at 155° W

and projection of predicted Hawaiian plume conduit
(red has source that moves freely, purple assumes fixed source)

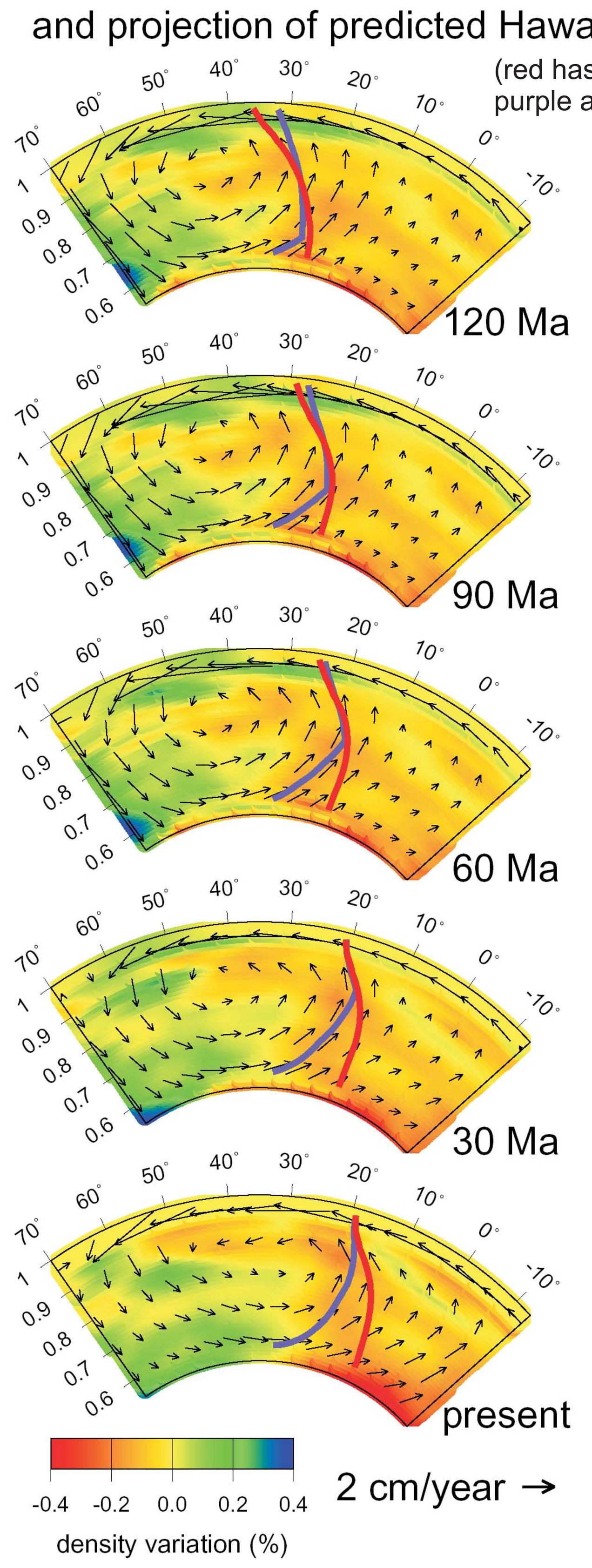

Step 1: density field inferred from seismic tomography (here: model *smean* by Becker and Boschi, 2002)
↑
compute flow with spectral method (*Hager and O'Connell, 1979, 1981*)
↑
backward advection for t < 68 Ma

also, plate motion b.c. for flow changes with time (for t < 120 Ma)

Step 2: insert vertical conduit (here: at time 170 Ma)
↓
plume conduit gets distorted
↓
hotspot moves